Laser Dynamics and Delayed Feedback

Kathy Lüdge[1] and Benjamin Lingnau[2]
[1]Institut für Theoretische Physik, Technische Universität Berlin, Berlin, Germany
[2]Department of Physics, University College Cork, Cork, Ireland

Article Outline

Glossary

Laser dynamics Time evolution of the laser light within the cavity as well as the time evolution of the charge-carriers that participate in the radiative emission process.

Constant wave emission (cw) Laser emission with a constant intensity.

Relaxation oscillations (RO) If a laser is perturbed from its steady state (constant wave emission), it will relax back performing a pure exponential decay (*Class-A* laser) or by performing damped oscillations (*Class-B* laser); damping rate and oscillation frequency are used to quantify the dynamics.

***Class-C* laser** A laser, for which the timescale of the induced material polarization inside the gain material is on the same order of magnitude as the electron and the photon lifetime. These lasers have to be modeled with Maxwell-Bloch equations in contrast to *Class A* and *Class B* lasers where laser rate-equations are sufficient for the modeling.

Bifurcation qualitative change in the system's behavior under parameter changes.

1D bifurcation diagram Unique extrema detected within a time series of the laser intensity, plotted as a function of one system parameter (bifurcation parameter) to detect bifurcations; e.g., suddenly occurring harmonic oscillations (Hopf bifurcation) or a sudden birth of new solutions (saddle node bifurcation).

2D bifurcation diagram Classification of the system dynamics in a 2D parameter space; bifurcations form the boundaries between parameter regions of qualitative different dynamics (e.g., chaotic pulsing and periodic oscillations).

External cavity mode (ECM) Optical mode that can exist in an optical resonator that is formed by a laser and an external cavity (laser with optical self-feedback); with increasing feedback strength the number of ECMs increases and their stability changes.

Definition of the Subject

The subject of investigating the laser dynamics under optical feedback is to characterize the changes in the light emission dynamics, i.e., unravel the bifurcation structure, when a laser is perturbed by its own back-reflections. Since optical feedback can happen due to unwanted reflections in every optical setup, it is important to note, at first, the tolerance of a stable laser to perturbations by optical feedback. Secondly, also complex pulsations and chaotic emission can be useful for applications and thus there is a need to understand the conditions for an emergence of complex laser dynamics. Mathematically the subject is interesting because the dynamics is modeled by delay differential equations, where the delay is given by the time the light needs to re-enter the cavity. In this entry, we will compare different semiconductor laser systems which are quantum dot (QD) and a quantum well

A. Hutt, H. Haken (eds.), *Synergetics*,
https://doi.org/10.1007/978-1-0716-0421-2_729

Originally published in
R. A. Meyers (ed.), *Encyclopedia of Complexity and Systems Science*, © Springer Science+Business Media LLC 2020
https://doi.org/10.1007/978-3-642-27737-5_729-1

(QW) lasers with one more wavelength emission as well as nanolaser systems with very short photon lifetimes (*Class – C* laser). We will learn the importance of internal timescales of the gain medium and give some general rules about how the internal degrees of freedom simplify the emerging light emission under optical feedback.

Introduction

The effect of delay has been investigated in various systems and recent progress in this field is documented for instance in focus issues on delay systems (Erneux et al. 2017; Otto et al. 2019). In this chapter, the focus lies on the laser dynamics when a control signal from the laser is fed back into it after a time delay. This includes setups such as external optical feedback, which can be realized, for example, by a simple mirror in some distance of the laser which feeds back the emitted light into the laser cavity. Another implementation is by an external electronic circuit which feeds back a delayed electric signal to the laser device depending on the output of the laser. In this context, the interaction between the laser and the feedback signal becomes increasingly complex when the feedback time is similar to the internal laser timescale. Since in real-world applications parasitic reflections off surfaces and optical interfaces can never be suppressed completely, time-delayed feedback arises naturally in nearly every laser setup. Immense effort has been put into improving the resistance of semiconductor lasers towards optical instabilities caused by feedback (Lenstra et al. 2019) in applications where a steady laser output is required. At the same time, the guided exploitation of feedback leads to novel applications harnessing the dynamical complexity of the system. In both cases, a thorough understanding of the underlying physical and dynamical processes is required.

The dynamical complexity of lasers with feedback is an extremely broad topic which has attracted much interest in the past and today. A lot has been done in order to understand the bifurcation structure of lasers with optical feedback and this entry does not aim to give a complete overview. The interested reader is referred to the pioneering works that can be found in Mørk et al. (1992), Sano (1994), Simmendinger and Hess (1996), Ye and Ohtsubo (1998), Ohtsubo (1999); Erneux et al. (2000), Pieroux et al. (2000, 2001), Wolfrum and Turaev (2002), Yanchuk and Wolfrum (2004), Radziunas et al. (2006), Rottschäfer and Krauskopf (2007). A variety of experimental data exists, see for example (Mørk et al. 1990a; Li et al. 1993; Heil et al. 2003; Wünsche et al. 2008; Kim et al. 2014; Locquet et al. 2017) or results on integrated devices (Kane et al. 2015; Karsaklian Dal et al. 2017) which support and still inspire theoretical analysis. See, e.g., (van Tartwijk and Agrawal 1998; Soriano et al. 2013; Ohtsubo 2013) for an overview. General properties of delay systems, like the recurrence of solutions (Yanchuk and Perlikowski 2009), play a crucial role to understand the response of a laser to delayed feedback.

In delayed feedback systems, the interplay with noise sources as they usually appear due to spontaneous photon emission can lead to a variety of dynamical effects and unforeseen behavior. This issue will only shortly be touched in the course of this entry and the interested reader is referred to the literature: The effect of noise was studied in Mørk et al. (1988a, 1990b) to explain mode hopping in multimode lasers with feedback, in Otto et al. (2014) to find coherence resonance, or in Oliver et al. (2015), Jüngling et al. (2018), Porte et al. (2014) to quantify the consistency properties of the laser output via the evaluation of the time delay signature (Rontani et al. 2007, 2009). Related to that the linewidth reduction with optical feedback has attracted recent interest as well (Agrawal 1984; Flunkert and Schöll 2007; Jaurigue et al. 2016; Brunner et al. 2017). The complex feedback induced dynamics that is the focus of this entry is usually detrimental to the linewidth (Li et al. 1993; Lenstra et al. 1985), but the bifurcation analysis that we present below can predict the regions where the feedback leads to a stabilization.

An important step towards improving the resistance of semiconductor lasers to optical feedback and other perturbations was the fabrication and subsequent employment of self-assembled semiconductor quantum dots (QDs) as the active medium in lasers (Bimberg et al. 1999; Bimberg

and Pohl 2011). In addition to their reduced threshold current and temperature stability, QD lasers are more robust against such perturbations (Otto et al. 2010, 2012a; Globisch et al. 2012; Lingnau et al. 2013; Duan et al. 2019; O'Brien et al. 2004; Huyet et al. 2004). As we will see later on, this robustness is facilitated by a change of the internal dynamical timescales due to the presence of the QDs.

In recent years there has been a steady push towards exploitation of complex dynamics induced by delayed feedback in laser systems. Right now those laser systems with delay find great attention in applications for information processing, i.e., all-optical reservoir computing (Argyris et al. 2018; Bueno et al. 2017; Kuriki et al. 2018; Nguimdo et al. 2017), as random number generators (Verschaffelt et al. 2017; Reidler et al. 2009; Oliver et al. 2011), in chaotic LIDAR systems (Lin and Liu 2004; Cheng et al. 2018), or in nanometric sensing (Choi et al. 2019).

This review article will discuss the interrelation between dynamic degrees of freedom within the laser gain medium and the stability of the laser if subjected to optical self-feedback. We will show that the response becomes less complex and more controllable with every additional timescale that is added to the system dynamics.

In the following, we will first introduce a rate equation model for nanostructured laser gain media in section "Dynamic Timescales and Relaxation Oscillations" and discuss the role of the charge carrier relaxation timescales that directly or indirectly participate in the laser process and, for their part, control the laser response to perturbations. Second, different semiconductor laser with complex gain media and their response to optical feedback will be compared in section "Optical Feedback (Class-B Lasers)" and the nonnegligible dynamic effect of a model reduction will be discussed. The effect of feedback on devices with nanoscale dimensions, where the photon lifetime starts to be on the same order of magnitude as the timescale of the microscopic polarization, will be discussed in section "Optical Feedback of Class-C Lasers" before we come to quantum dot lasers with simultaneous two-color emission and their response to feedback in section "Optical Feedback of Two-State QD Lasers."

Dynamic Timescales and Relaxation Oscillations

The response of dynamical systems towards perturbations depends sensitively on the internal dynamical timescales of the system itself. A universal example of this is a driven damped oscillator, showing resonance effects when driven close to its natural frequency, with the resonance overshoot depending on its damping. Most semiconductor lasers possess an intrinsic resonance frequency and associated damping due to the presence of relaxation oscillations (ROs) – oscillations in the energy exchange between the intracavity photons and the available gain. In the laser classification scheme due to Arecchi et al. (1984), such lasers are labeled *Class-B*. These intrinsic timescales can be readily observed in the laser response to delayed feedback. Most dynamical features occur at frequencies related to the RO frequency, and complex dynamics can be observed if the delay time is in the order of the RO frequency. The minimum feedback strength required to induce complex dynamics is closely related to the damping of the ROs, with stronger damping usually leading to a more robust system (Helms and Petermann 1990). It is therefore natural to assume that the introduction of additional timescales into a dynamical system that is subjected to delayed feedback changes its response. We want to illuminate this effect for two examples: At first, a QD laser that has more than one carrier type and thus an additional relaxation channel with an associated dynamic timescale. Secondly, a *Class-C* laser where the timescale of the induced material polarization plays a crucial role for the dynamics.

Quantum-dot lasers differ from conventional semiconductor lasers in the dimensionality of the active medium. Whereas in quantum-well lasers the active medium is quasi-two-dimensional, QDs are effectively zero-dimensional systems, embedded in a two-dimensional charge-carrier reservoir. The active optical transition is thus formed by deeper lying atom-like energy states which have to be gradually filled by surrounding charge-carriers, see Fig. 1a. This additional scattering pathway introduces an extra timescale in the dynamic laser system (Table 1).

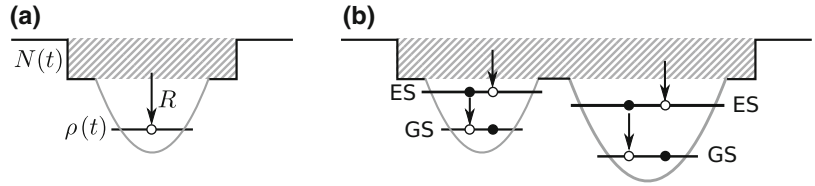

Laser Dynamics and Delayed Feedback, Fig. 1 (**a**) Sketch of the energy levels in the simplest quantum-dot (QD) laser. The QD occupation probability ρ increases due to inscattering of charge carriers from the reservoir states, N, with the scattering rate R. The QD transitions are the active optical transitions. (**b**) More realistic depiction of the quantum dot structure. Quantum dots with different sizes have different energy levels. In addition to the ground state (GS), one or more excited states (ES) can exist

The minimal model to describe a QD laser is thus at least three-dimensional, as we need to consider the dynamics of the charge-carrier number in the reservoir, $N(t)$, the occupation of the QD states, $\rho(t)$, and the amplitude of the cavity electric field, $E(t)$ (the intracavity photon number is proportional to $|E(t)|^2$):

$$\dot{N} = J - \frac{N}{T_1} - R\left(\rho^{\mathrm{th}} + d\left(N - N^{\mathrm{th}}\right) - \rho\right), \quad (1a)$$

$$\dot{\rho} = R\left(\rho^{\mathrm{th}} + d\left(N - N^{\mathrm{th}}\right) - \rho\right) - \frac{\rho}{T_{\mathrm{sp}}} - \left[g\left(\rho - \rho^{\mathrm{th}}\right) + \frac{1}{T_{\mathrm{ph}}}\right]|E|^2, \quad (1b)$$

$$\dot{E} = \frac{g}{2}(1 - i\alpha)\left(\rho - \rho^{\mathrm{th}}\right)E + \frac{K}{T_{\mathrm{ph}}}e^{-iC}E(t - \tau) \quad (1c)$$

The parameters entering the equations are explained in Table 1. In thermodynamic equilibrium, the in- and out-scattering processes between charge carrier states at different energies obey a detailed-balance relation, i.e., their ratio is given by a Boltzmann factor that determines the equilibrium occupation of the charge-carrier states. For the quasi-equilibrium within a pumped laser, this also applies and in the presented minimal QD laser model it enters via the coefficient d. The coefficient $d = \frac{\partial}{\partial N}\rho^{\mathrm{eq}}\big|_{\mathrm{th}}$ describes the change of the quasi-equilibrium QD occupation with respect to the normalized reservoir density close to the threshold. With increasing charge-carrier number in the reservoir, this balance is shifted towards higher occupation, which is included in the minimal QD laser model in a linearized fashion. An important feature of QD lasers is the imperfect clamping of charge-carriers above threshold (Lüdge and Schöll 2009; Röhm et al. 2015), i.e., the quantum dots can never be filled completely.

Laser Dynamics and Delayed Feedback, Table 1 Parameters used in this chapter and their meaning

Symbol	Meaning
J	Normalized pump current
T_1	Charge-carrier lifetime
T_2	Induced polarization lifetime
T_{ph}	Cavity photon lifetime
T_{sp}	QD lifetime
R	QD scattering rate
N^{th}	Threshold reservoir density
ρ^{th}	Threshold QD occupation probability
d	Detailed balance coefficient
g	Normalized gain coefficient
α	Amplitude-phase coupling parameter
K	Optical feedback strength
C	Feedback phase
τ	Feedback delay time

The delayed optical feedback enters the equations via the delayed optical field, $E(t - \tau)$ in Eq. (1c). This modeling approach was first proposed independently by Rosanov (1975), and Lang and Kobayashi (1980). Within this approach, only a single round-trip in the external cavity formed between the laser facet and the external mirror is taken into account. For strong external reflectivities, multiple round-trips become important and the treatment of the feedback field must be

extended (Schelte et al. 2019). The optical feedback is characterized by the feedback strength K, the time delay τ, and the feedback phase C. The effect of the feedback and the effect of α will be discussed in the next section. For now we set $K = 0$ which completely decouples the dynamics of the phase of the electric field and leaves the intensity $|E(t)|^2$ as the only important dynamic quantity for the field inside the cavity.

Depending on size and composition of the QDs, the effective charge-carrier scattering rate R can vary significantly. We therefore treat it as a free parameter and discuss its impact on the dynamic response of the QD laser in Fig. 2. This allows us to identify different dynamic regimes and the important dynamic timescales of a QD laser system, Eq. (1a–1c), as a function of R. The internal timescales and frequencies can be extracted from the Lyapunov exponents, which are the eigenvalues of the Jacobian of the right hand side of the differential equation system. Real and imaginary part of the dominating eigenvalue λ determine the respective intrinsic relaxation oscillation frequencies and damping rates, i.e., Im $\lambda = \omega_{RO}$ and Re $\lambda = \Gamma_{RO}$. Figure 2 shows their dependence on the scattering timescale R. As can be seen, the presence of the additional scattering process strongly influences the RO timescales. The most striking feature is the maximum of the RO damping and the vanishing RO frequency at values of $R \approx 10^{11}\ s^{-1}$. For these moderate scattering rates,

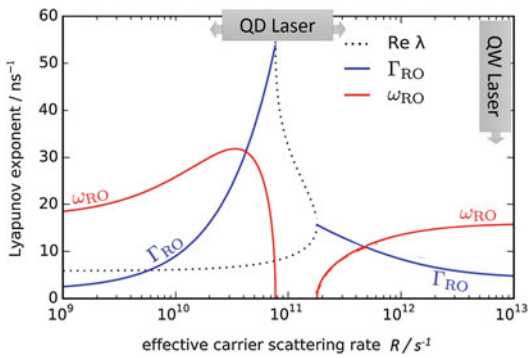

Laser Dynamics and Delayed Feedback, Fig. 2 Relaxation oscillation damping Γ_{RO} (blue) and frequency ω_{RO} (blue) determined from the minimal QD laser model given in Eq. (1a–1c). (Reproduced from Lingnau (2015) with permission from Springer)

the ROs are overdamped and the eigenvalues become purely real. For higher values, both charge-carrier types are closely coupled and the dynamics has only one effective degree of freedom in the charge-carrier dynamics. For much smaller values of R, the carrier reservoir N is only weakly influenced by the dynamics of ρ and remains nearly constant. Thus, it acts as a constant reservoir for the active charge-carriers and again the charge-carrier dynamics is effectively one-dimensional. In the intermediate range of R, where we cannot neglect the dynamics of either charge-carrier species, the internal gain dynamics is more complex but leads to a very simple dynamic response, i.e., without visible relaxation oscillations. At the same time, the RO damping is largest close to this parameter range, which explains the resilience of QD lasers towards external perturbations. This is usually known for *Class-A* lasers, which however do not have any independent degree of freedom of the carrier dynamics. While we have explicitly discussed the case of a QD laser, we note that in most cases an additional slow dynamic scattering or charge-carrier transport process will lead to dynamic equations similar to Eq. (1a–1c). The presence of such a slow dynamic charge-carrier process will thus lead to similar dynamic behavior.

As we will see, the laser response to delayed optical feedback is not as complex in QD lasers as in quantum-well (QW) lasers. QW lasers can be thought of to operate in the limit of $R \to \infty$, with only one type of charge-carriers present and a near-instant equilibration. In this limit, the minimal QD laser model reduces to the QW laser equations:

$$\dot{N} = J - \frac{N}{T_1} - \left[g\left(N - N^{th}\right) + \frac{1}{T_{\mathrm{ph}}}\right]|E|^2 \quad (2a)$$

$$\dot{E} = \frac{g}{2}(1 - i\alpha)\left(N - N^{th}\right)E + \frac{K}{T_{\mathrm{ph}}}e^{-iC}E(t-\tau) \quad (2b)$$

These equations are of Rosanov-Lang-Kobayashi-type, and they constitute the fundamental model for the description of *Class-B* lasers with weak time-delayed optical feedback.

Optical Feedback (Class-B Lasers)

As already mentioned in the last section, the most important timescale when it comes to the response of a laser gain medium to optical perturbations is the relaxation oscillation frequency and damping, as they describe how the laser relaxes to its steady state. While a *Class-A* laser just reacts with an exponential decay of its intensity, the so-called *Class-B* laser performs damped oscillations towards the steady state. We now illuminate three examples of semiconductor lasers: A conventional quantum well (QW) laser (*Class-B*) with one carrier type as given in Eq. (2a–2b); a quantum dot (QD) laser that has more than one carrier type and thus an additional dynamic degrees of freedom and is described by the minimal model in Eq. (1a–1c) and a QD laser that is described on a different more complex level of the laser modeling hierarchy.

The time-delayed feedback term introduced already in the last section will now be discussed in detail. A sketch of the setup is shown in Fig. 3. For coherent optical feedback, the response will depend on the phase of the electric field. The feedback phase C gives the optical phase shift accumulated over one feedback round-trip time and determines whether the light fed back into the laser interferes destructively or constructively with the cavity field. The dynamics under time delayed optical feedback has been shown to sensitively depend on the feedback phase, especially in the regime of short delays (Heil et al. 2003) which we assume in this entry. Short delay, in this context means that the roundtrip time in the external cavity τ is not larger than the RO period $T = 2\pi/\omega_{RO}$. The most general formulation of the dynamic equation of the electric field then reads (van Tartwijk and Agrawal 1998; Lingnau et al. 2012, 2013):

$$\dot{E}(t) = \left[G(\omega, t) - i\Delta\omega_0 - \frac{1}{2T_{\text{ph}}}\right]E(t) + \frac{K}{T_{ph}}e^{-iC}E(t-\tau), \tag{3}$$

where $K \in [0, 1]$ is the feedback strength, denoting the ratio of the light lost through the cavity mirrors that is coupled back into the cavity. The electric field is expressed in a rotating frame with frequency $\Delta\omega_0$, such that its phase velocity vanishes in the steady-state. The external cavity feedback time τ and the feedback phase C are in principle both determined from the optical path length of the feedback section, but since the feedback phase is much more sensitive to changes in τ, it is treated as an independent parameter (Heil et al. 2003). The gain $G(\boldsymbol{\omega}, t)$ is in general a complex valued function determined by the microscopic polarization of the gain medium. Its real part, $\text{Re}[G(\boldsymbol{\omega}, t)]$, describes the amplitude gain of the electric field, and $\text{Im}[G(\boldsymbol{\omega}, t)]$ is the change of the instantaneous electric field frequency due to carrier-induced refractive index changes. The modeling of $G(\boldsymbol{\omega}, t)$ can be performed on different levels of complexity. Very common is the introduction of an amplitude-phase coupling or Henry parameter, α, which describes the instantaneous coupling of the electric field frequency to the optical gain. The amplitude phase coupling factor α is defined as

$$\alpha = -\frac{\partial \text{Im}[G(\boldsymbol{\omega})]/\partial N}{\partial\, \text{Re}\,[G(\boldsymbol{\omega})]/\partial N} \tag{4}$$

and significantly simplifies the dependence of the complex gain $G = \text{Re}\ G + i\text{Im}\ G$ on the carrier density N. The simplified dynamic equation for the electric field then reads (van Tartwijk and Agrawal 1998; Ohtsubo 2013; Lingnau et al. 2013):

$$\dot{E}(t) = \left[\text{Re}\ G(\omega) - \frac{1}{2T_{\text{ph}}}\right](1 - i\alpha)E(t) + \frac{K}{T_{\text{ph}}}e^{-iC}E(t-\tau). \tag{5}$$

The amplitude phase coupling is an important parameter when discussing the sensitivity of the laser to optical feedback and for determining the

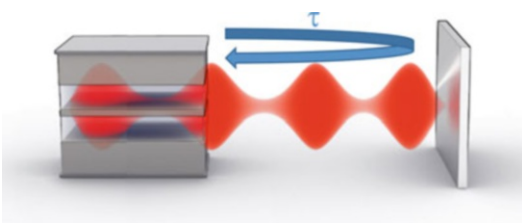

Laser Dynamics and Delayed Feedback, Fig. 3 Sketch of a semiconductor laser that is subjected to optical self-feedback with a delay length of τ

structure of the dynamical solutions. High values of α generally lead to highly complex dynamics. The general solution structure of the laser with delayed optical feedback is largely formed by the so-called external-cavity modes (ECMs). These modes denote the solutions of the combined system of the laser and the external cavity with constant intensity. The resonant frequencies of the isolated laser cavity and the external cavity are in general different. The presence of the feedback thus introduces a frequency shift of the laser output away from the free-running lasing frequency. The ECM solutions of the form $E(t) = E_0 e^{-\Omega t}$ are located on an ellipse in the phase space spanned by the optical gain ReG and the ECM frequency, Ω, as we will discuss further in section "Optical Feedback of Class-C Lasers." If the gain is assumed to be linear, i.e., Re $G = g(N - N^{th})$, which is a common and very good assumption for laser operation (van Tartwijk and Agrawal 1998; Ohtsubo 2013; Mørk et al. 1988a; Chow and Koch 1999), the charge-carrier number N and Ω can be used for the phase space projection of the ellipse.

The dynamics of the complex gain G in a QW laser with a gain medium consisting of only one carrier type (same dynamics as observed from the minimal QD laser model Eq. (1a–1c) for large R) can be closely described by a constant α. The induced frequency shift then proportionally and instantly follows the dynamics of the optical gain. In a QD laser with finite R, both resonant and nonresonant carriers within different states must be considered, and thus the gain dynamics are more complex due to the additional dynamic degrees of freedom. The minimal QD laser model takes the dynamics of the nonresonant carriers into account but still assumes an α-factor for the refractive index changes. Figure 4 compares the reaction to feedback for both laser types. There, the bifurcation diagram, i.e., the unique extrema found in a time series of the laser intensity for a given feedback strength K, is displayed as a function of K. Additionally, two timeseries are plotted as insets in Fig. 4b which illustrate the increase in complexity with K. Comparing both bifurcation diagrams of the QW and the QD laser, it can be seen that the differences in the charge-carrier dynamics directly influence the dynamics.

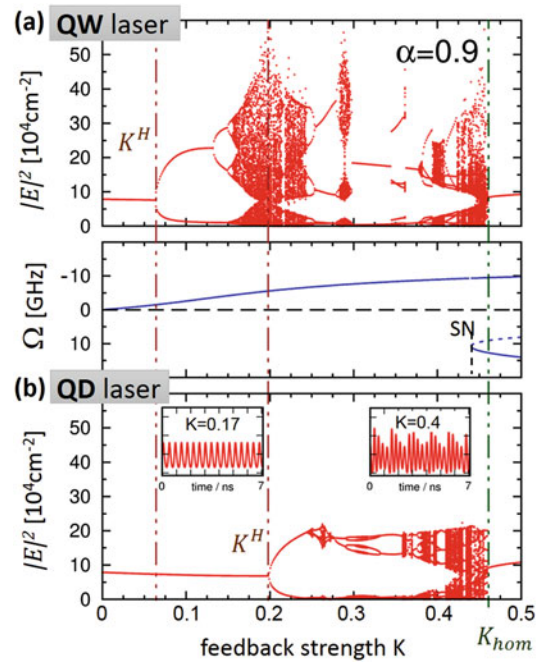

Laser Dynamics and Delayed Feedback, Fig. 4 1D-Bifurcation diagram of two different lasers if subjected to optical self-feedback. It shows the impact of different RO damping exemplarily for a QW laser (**a**) and a QD laser (**b**). Insets in (**b**) show time series of the QD laser for two K values. Vertical dash-dotted lines indicate the critical feedback strength K^H and the homoclinic bifurcation K_{hom}. *SN* indicates the saddle-node bifurcation where new ECM solutions (one stable and one unstable) are born. $C = \pi$, $\tau = 160$ ps. (Reproduced from Otto et al. (2010) with permission from Wiley)

The most significant difference is the value of the feedback strength K at which the laser starts to show intensity oscillations. This bifurcation point is the critical feedback strength. It is labeled K^H in Fig. 4. It is much larger for the QD laser, which means this laser can withstand a higher amount of feedback before it starts to show intensity oscillations. Instead, the point where the two lasers switch back to stable emission on the next ECM solution via a homoclinic bifurcation at K_{hom} only marginally depends on the gain model (vertical dash-dotted line in Fig. 4). The reason lies in the solution structure formed by the ECMs of the electric field equation which are also plotted as blue lines in Fig. 4 (center). At a K value of 0.45 two new ECM solutions appear: one stable (solid line) and one unstable (dashed). This bifurcation point is called saddle node bifurcation and

indicated with *SN* in Fig. 4 (center). The ECM solutions themselves are the same for both lasers, as long as they have the same α-factor, while the instability of the first solution (the Hopf bifurcation at K^H) strongly depends on the relaxation oscillation timescales and thus on the internal carrier dynamics. It can be analytically shown (Otto et al. 2012a, b; Globisch et al. 2012) that the critical feedback strength K^H, i.e., the Hopf bifurcation point at which the stable ECM with frequency Ω is destabilized, can be approximated via:

$$K^H = \frac{2\Gamma^{RO} T_{\mathrm{ph}}}{\sqrt{1+\alpha^2}\,(1-\cos(\omega^{RO}\tau))\cos(\pi - C - \Omega\tau + \arctan(\alpha))} \tag{6}$$

Here, ω^{RO} is the frequency of the relaxation oscillations and Γ^{RO} their damping rate. Similar equations for the critical feedback level have already been derived in Helms and Petermann (1990), Mørk et al. (1988b), Binder and Cormack (1989), however, without treating the dependence on the feedback phase. For long feedback delay, the phase is hard to control. It is therefore useful to estimate the smallest value of K^H (C) which is reached for $C = -\Omega\tau + \pi + \arctan\alpha \approx \pi + \arctan\alpha$ (see for example Fig. 5 for the evolution of the stability border, i.e., transition from blue to white, as a function of C). Thus, the laser is guaranteed to be stable for

$$K^H < K^H_m = \frac{\Gamma^{RO} T_{\mathrm{ph}}}{\sqrt{1+\alpha^2}}. \tag{7}$$

This stability condition was derived for a quantum-well laser by Mørk et al. (1992) and previously suggested by Helms and Petermann (1990) as a simple analytical criterion for tolerance with respect to optical feedback. If the laser operates at the minimum linewidth mode (Levine et al. 1995), a slightly different minimal critical feedback strength is derived from Eq. (6) and is given by $K^H_m = \Gamma^{RO} T_{\mathrm{ph}} \sqrt{1+\alpha^2}/(\alpha^2 - 1)$.

From Eqs. (6) and (7), it becomes clear that the less complex QW laser with its small RO damping is more susceptible to back reflections while a QD laser, engineered such that it shows very strong RO damping, has a very high feedback tolerance.

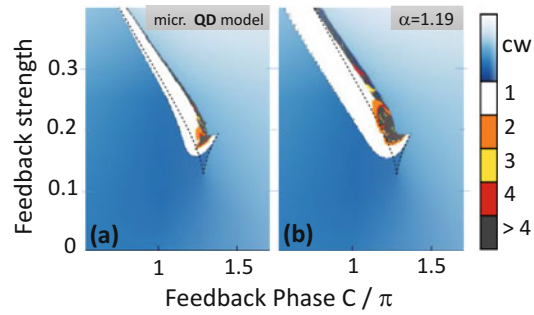

Laser Dynamics and Delayed Feedback, Fig. 5 Comparison of the feedback induced dynamics for a full microscopic QD laser model (Lingnau et al. 2013) with many degrees of freedom of the charge carriers (**a**) and the corresponding QD laser model that uses an effective α-factor description (**b**). The blue color encodes the intensity of the stable laser emission while other colors indicate the number of unique maxima observed in the pulsating time series. Dashed lines represent the saddle-node (SN) bifurcation along which a new ECM solution is born. $\tau = 100\ ps$

For the latter, all involved carriers relax on similar timescale and the number of dynamic degrees of freedom is higher.

The numerical and analytical results on the QD laser presented so far have been obtained for the minimal model shown in Eq. (1a–1c) with two carrier types, N and ρ. If a more sophisticated modeling approach is chosen, the equations can be extended to a more microscopic model with a higher number of degrees of freedom of the carriers. The details are discussed in Lingnau et al. (2013) and we just mention some important ingredients. Besides the pure existence of more confined carrier levels and thus more dynamic equations, this model also considers dynamic changes in the imaginary part of the material gain Im G, i.e., the refractive index can show dynamics on its own timescale. Surprisingly, the QD laser that is described by the much more complex model shows less complex response to optical feedback. This is visualized in Fig. 5a, b where the laser dynamics numerically obtained from the microscopic model and the minimal model with constant α-factor are compared. The dashed lines in Fig. 5 represent the saddle-node (SN) bifurcation along which a new ECM solution

is born. The critical feedback strength where the first ECM loses stability can be seen along the transition from blue (cw operation) to white areas (regular pulsations with one maximum). It can be seen that taking into account the contribution of the refractive index dynamics in (a) leads to a stabilization of the dynamics and consequently less regions with complex dynamics (orange and grey colors) occur. If the charge-carrier induced frequency shift is approximated by an α-factor as done in (b) (compare also Eqs. (3) and (5)), the separate time evolution of the imaginary part of the gain is neglected, and the gain dynamics becomes less complex. As a result, however, the dynamic response to optical feedback becomes more complex (Fig. 5b) and we instead observe a simplification of the dynamic response for the higher internal complexity (Fig. 5a). The effect of increasing the susceptibility to optical perturbations by a model reduction occurs to be rather general and has to be kept in mind.

At the borders between stable emission and regions with complex dynamics (between blue and grey in Fig. 5), bifurcations occur and the laser switches to emission at the next ECM, i.e., emission at a different wavelength. For the pump current chosen here this is a homoclinic bifurcation. This transition was already mentioned in Fig. 4 and marked with K_{hom}. It defines the point in parameter space where the laser re-stabilizes. Around this transition point where the laser just started to emit at the new frequency, the *cw* solution is only weakly stable and thus very susceptible to noise. To get an impression of the dynamics in phase space, Fig. 6a, b visualizes the trajectory after a noise perturbation in the vicinity of the homoclinic bifurcation. These noise-induced pulsations are no stable solutions of the delay differential equation but they follow parts of an attractor that has been stable before. As such the interspike interval between pulses, indicated by T_{ISI} in Fig. 6a, changes stochastically. Interestingly an optimal noise strength can be found, where the noise-induced pulsations occur most regularly, i.e., the distribution of interspike intervals T_{ISI} becomes relatively sharp. This effect – called coherence resonance – occurs due to the nonlinearity of the light-matter interaction and is a universal effect in excitable nonlinear systems in the presence of noise (Lindner et al. 2004). Experimentally, these kind of pulses have been observed, e.g., in Heil et al. (2003, 2001). Note that for higher laser pump currents, the bifurcation that causes the laser to start stable emission at the newly born ECM changes from a homoclinic bifurcation to a boundary crisis (Otto et al.

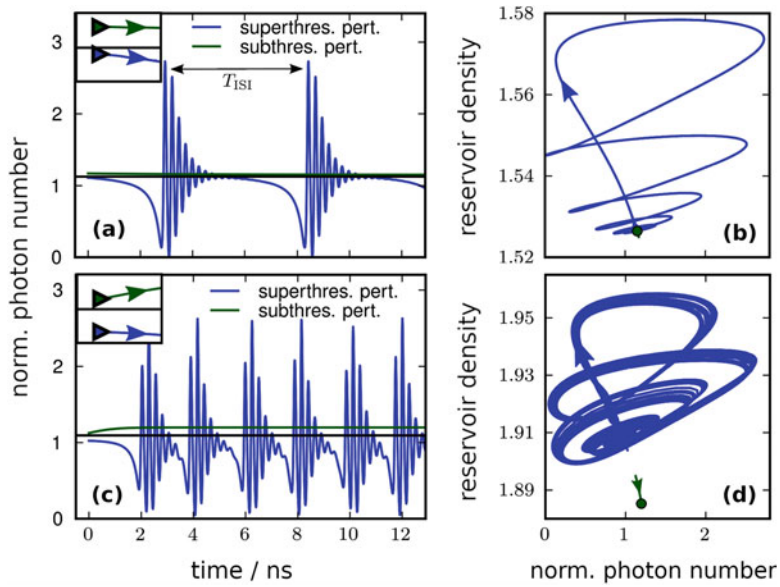

Laser Dynamics and Delayed Feedback, Fig. 6 Trajectories of a QD laser with optical feedback after noise excitation plotted as a function of time (**a**, **c**) and as a phase space projection (**b**, **d**). (**a**, **b**): close to the homoclinic bifurcation that was discussed in Fig. 4;(**c**, **d**): close to the boundary crisis that exists for higher pump currents. $C = \pi$, $\tau = 160\,ps$. (Reprinted with permission from Otto et al. (2014) ©The Optical Society)

2014). Nevertheless, coherence resonance can also be found here (Otto et al. 2014). Figure 6c shows the chaotic pulse packages induced by a superthreshold perturbation right after the boundary crisis of the chaotic attractor. The green circle in Fig. 6d indicates the stable ECM solution that is perturbed by the noise. The path of the trajectory along the former chaotic attractor can be seen in the phase space projection in Fig. 6d.

Optical Feedback of Class-C Lasers

So far the discussion was limited to *Class-B* lasers that were solely described by the carrier and photon dynamics. However, the light matter interaction is driven via the microscopic polarization within the medium. For the *Class-B* laser, the optical gain is assumed to instantaneously follow the available charge-carriers in the optically active transitions. The stimulated emission rate is assumed to adiabatically follow the charge-carrier and electric field dynamics and thus does not need to be explicitly considered as a dynamical variable. With the recent success and progress of semiconductor epitaxy and wafer processing, the realization of very small devices has become possible, down to lasers with cavity dimensions in the order of the wavelength of the laser light. Due to the small size of their cavity, those nanolasers have a strong spontaneous emission and relatively short photon lifetimes. While the stronger photon losses are compensated by an increase of the optical gain, the photon lifetime now is comparable to the lifetime of the induced material polarization. The active laser medium can thus no longer be treated as a simple source of instantaneous optical gain. Rather, the field emitted by stimulated emission of light becomes a dynamical variable itself. When all three timescales (electrons, polarization, photons) end up to be of a similar order of magnitude, the fundamental physics of the laser system change. These nanolasers, so-called *Class-C* lasers, exhibit special behavior like the second laser threshold (Haken 1986), after which self-pulsing of the laser emission occurs, but also react differently to optical feedback (Lingnau et al. 2019).

Class-C lasers can be described by the Maxwell-Bloch equations (MBEs), which explicitly include the dynamics of the induced material polarization (Chow and Koch 1999; Haken 1986). The delayed optical feedback extends the MBEs by an additional driving term in the electric field to include the effects of time-delayed optical feedback. Since we now want to focus on the effect of the polarization, a QW laser with just one carrier type N is modeled.

The normalized MBEs with delayed optical feedback are given by:

$$\dot{N} = \frac{1}{T_1}(J - N - 2c\,\mathrm{Re}\,[PE^*]), \tag{8}$$

$$\dot{P} = \frac{1}{T_2}[EN - (1 - i\alpha)P] - i\omega_0 P, \tag{9}$$

$$\dot{E} = \frac{1}{T_{\mathrm{ph}}}\left[cP - \frac{1}{2}E\right] - i\omega_0 E + \frac{K}{T_{\mathrm{ph}}}e^{-iC}E(t-\tau). \tag{10}$$

Here, the additional timescale T_2 of the induced polarization enters the equations. The stimulated emission is now given by cP, with a normalization constant $c = 1 + (2\alpha/(2 + T_2/T_{\mathrm{ph}}))^2$. The parameter α in Eq. (9) measures the frequency difference between the gain maximum and the cavity mode. For the case of very small T_2, when the MBE model reduces to the $Class - B$ laser model, it takes the role of the α-factor that we introduced in the last section.

The lifetime T_2 of the polarization plays a crucial physical role as it determines the gain bandwidth of the laser transition, with long lifetimes producing a sharp, narrow gain peak. Consequently, with increasing T_2 the gain bandwidth becomes narrower and the possible deviation of the lasing frequency from the transition frequency is limited. This reduces the number of possible ECMs in *Class-C* lasers with a single optical transition. It is depicted in Fig. 7 for four different values of the dephasing time T_2, which is the lifetime of the polarization. The rotating wave solutions of the above equation, i.e., the external cavity modes (ECMs), are shown as open circles in the plane of charge-carrier number, N, and ECM frequency, Ω. It underlines the impact of the additional dynamic equation and it can be seen that for $T_2 = 0$ we recover the case of a *Class-B* laser and

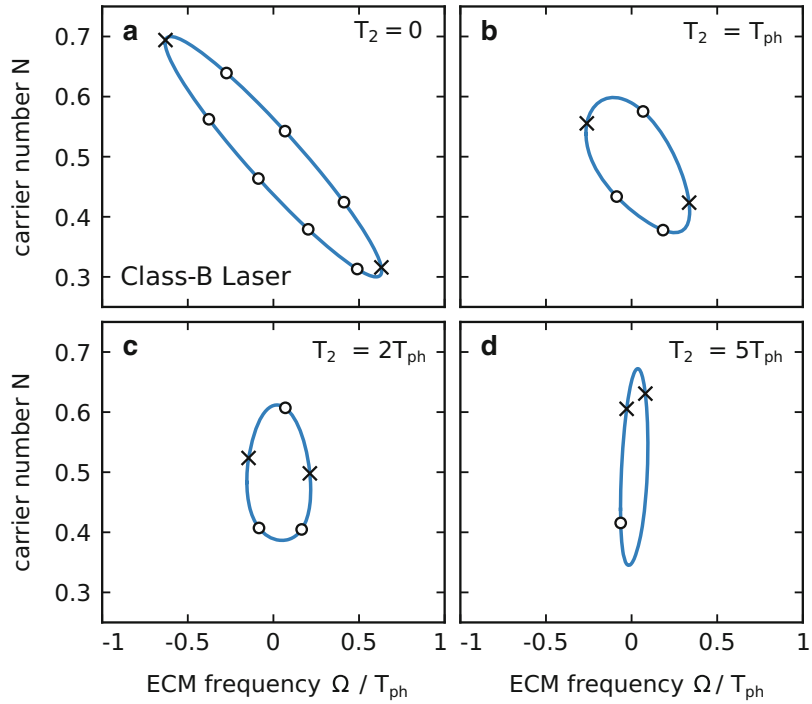

Laser Dynamics and Delayed Feedback, Fig. 7 External cavity solutions (ECMs) of a laser with optical self-feedback plotted as a function of ECM frequency Ω and carrier number *N*. (**a**) *Class-B* laser with dephasing times $T_2 = 0$, (**b**–**d**): *Class-C* laser $T_2 = T_{ph}$, $T_2 = 2T_{ph}$, and $T_2 = 5\ T_{ph}$. Solid closed lines denote all possible solutions in the (Ω, *N*)-plane while open circles denote solutions obtained for a specific feedback phase $C = \pi$. Crosses mark saddle node (SN) bifurcations where new solutions are born. The connection between the crosses separates the ellipse into regions where the solutions are born unstable (upper part) and stable (lower part). Other parameters: $K = 0.2$, $\tau = 20T_{ph}$, $\alpha = 3$. (Reprinted from Lingnau et al. (2019) with permission from Royal Soc)

observe the rotated ellipse in phase space on which the ECM solutions can exist. For larger values of T_2, the number of solutions (open circles) is decreased while they all move closer together. Furthermore, the effect of the amplitude-phase coupling α, which usually leads to a high aspect ratio of the ellipse for the *Class – B* laser, is reduced as can be seen by comparing the circles in Fig. 7. The possible ECM solutions appear in a more symmetric shape around $\Omega = 0$ for larger T_2 times.

The numerically obtained response of the *Class-C* laser to optical feedback is plotted in Fig. 8 for the four different dephasing times T_2. The number of unique maxima is encoded in the color and thus dark colors indicate complex dynamics and chaos. While a *Class-C* laser is usually known for its second laser threshold after which it emits chaotic light without any perturbations, it appears to be much more stable than a *Class-B* laser if it is subjected to optical feedback (compare Fig. 8a, d).

In the limit of $T_2 \to 0$ (Fig. 8a), the MBEs reduce to the conventional Lang-Kobayashi equations, which show well-known bifurcation cascades and eventually can produce optical chaos. For this case we also plotted the two bifurcations that organize the parameter space in Fig. 8a; the Hopf bifurcation at which the first ECM destabilizes, called critical feedback strength in section "Optical Feedback (Class-B Lasers)," is plotted in blue. The saddle node (SN) bifurcation where the next ECM is born (compare Fig. 4 (center) where the SN bifurcation is marked) is plotted in red. For higher values of T_2, the dynamical regions in the feedback parameter undergo a transformation.

Quite counter-intuitively, the addition of another dynamic dimension to the system can have a stabilizing effect on its dynamics. This

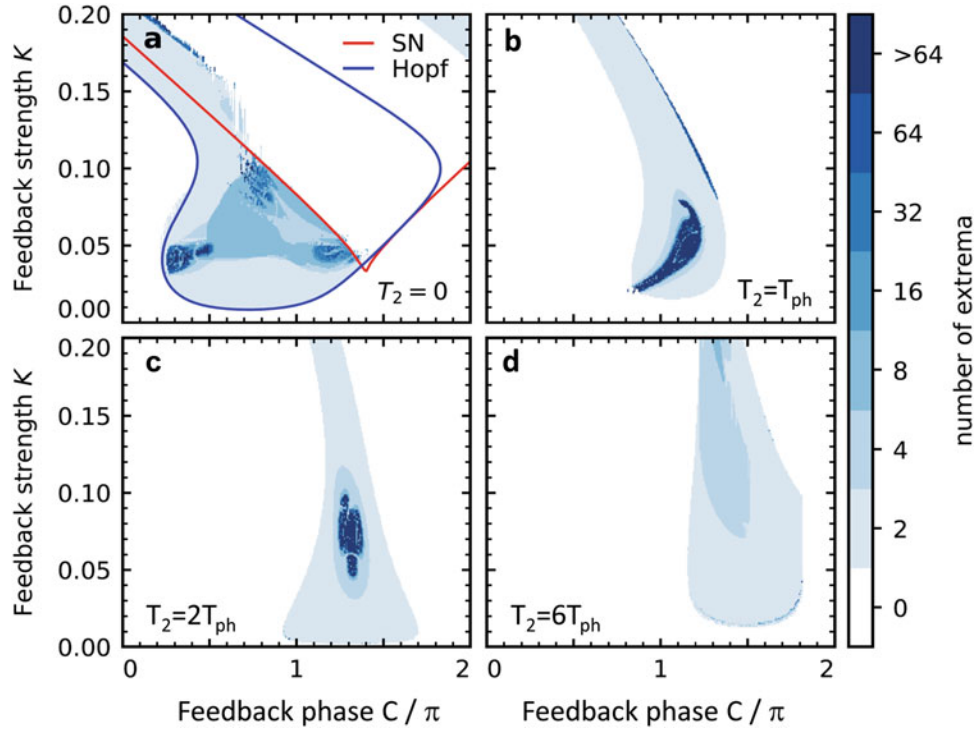

Laser Dynamics and Delayed Feedback, Fig. 8 Dynamics observed numerically in the laser emission for a small feedback delay time $\tau = 10T_{\mathrm{ph}}$ in the plane of feedback strength K and feedback phase C. (**a**): *Class-B* laser with $T_2 = 0$, (**b**–**d**): *Class-C* laser with $T_2 = T_{ph}$, $T_2 = 2T_{ph}$, and $T_2 = 6T_{ph}$. Shown are the number of unique intensity extrema (color-coded), where zero extrema correspond to CW operation, and nonzero values to periodic or complex dynamics. In panel (**a**), we show saddle-node (SN, red line) and Hopf (blue line) bifurcation curves of the first ECM, obtained by numerical path continuation. Other parameters: $J = 5$, $\alpha = 3$. (Adapted from Lingnau et al. (2019) with permission from Royal Soc)

can be seen for increasing values of T_2, for which the dynamics becomes strikingly less complex, and only small regions of chaos remain (see Fig. 8c, d). Following the arguments of the last sections, the explanation again lies in the increased dynamic degrees of freedom. Having the possibility for a dynamic response with independent polarization dynamics, a chaotic response becomes unlikely (Fig. 8d). Driving a dynamic system into chaos with external perturbations can thus be seen to become harder with higher phase space dimension which vary on a dynamic timescale similar to the rest of the system. This conclusion is found to be quite robust with respect to parameter changes.

To get some insights into the impact of the delay time τ, we visualize the dynamics of the $Class - C$ laser in another parameter plane spanned by T_2 and the delay time τ in Fig. 9a. Again the dark colors represent a high number of different maxima observed in the timeseries and thus more complex dynamics. As expected, small values of T_2 reproduce the dynamics of a *Class-B* laser and we find complex dynamics. Between $0.5\ T_{\mathrm{ph}} < T_2 < 2T_{\mathrm{ph}}$ only continuous wave or periodic emission is found, while dynamics with a higher number of unique maxima appears again for larger values of T_2. A high number of unique extrema is not sufficient to classify the dynamics into (quasi-)periodic or chaotic behavior. We therefore calculate the largest nontrivial Lyapunov exponent which gives us a value for the speed at which two adjacent trajectories diverge in time. A Lyapunov exponent with a positive value (plotted in red in Fig. 9b) indicates chaos (sensitive dependence on initial conditions), while negative values indicate stable dynamics. A value of zero is an indication for a periodic solution. We can thus conclude from

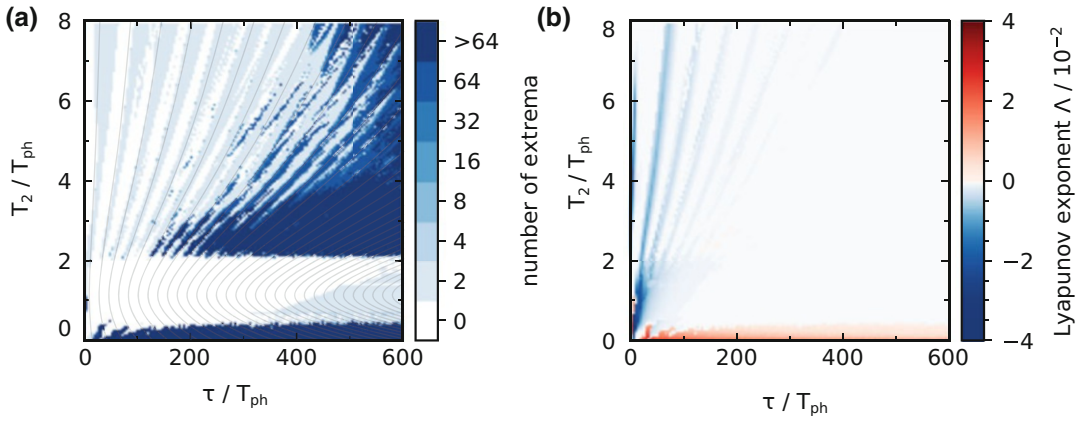

Laser Dynamics and Delayed Feedback, Fig. 9 Dynamics of a *Class-C* laser in dependence of the feedback delay time τ and the polarization dephasing time T_2. (**a**) Color code represents the number of unique extrema, thin grey lines show resonances of the relaxation oscillation frequency, $\tau = \left(n + \frac{1}{2}\right) \frac{2\pi}{|\mathrm{Im}\lambda|}$, with $n \in \mathbb{N}$. (**b**) largest Lyapunov exponent Λ. Other parameters: $J = 10$, $\alpha = 3$, $K = 0.1$, $C = \pi$. (Adapted from Lingnau et al. (2019) with permission from Royal Soc)

Fig. 9 that optical chaos only occurs for the *Class-B* laser case, mainly for high feedback delay times τ, while *Class-C* laser remain stable or, for large dephasing times, show quasi-periodic dynamics.

Optical Feedback of Two-State QD Lasers

Semiconductor lasers which are emitting on two distinct laser modes are a highly attractive application of laser dynamics due to the interaction of those modes. Prime examples of such laser systems include vertical-cavity surface emitting lasers (VCSELs), which due to their circular cavity symmetry support two orthogonally polarized modes (Olejniczak et al. 2009; Virte et al. 2012), or carefully designed laser cavity emitting on more than one wavelength (Osborne et al. 2009, 2012). Such two-mode lasers show a variety of complex dynamics related to the switching between the two laser modes in various setups including when subjected to time-delayed feedback (Osborne et al. 2012; Sciamanna et al. 2003). Their dynamics is governed by the energy exchange and gain competition between the two modes, which can be influenced by the external perturbation. Different realizations of two (or multi) mode emission will therefore show very similar properties, regardless of the exact system. We want to focus on two-mode emission with delayed optical feedback in this last section.

Quantum-dot lasers have shown two-state emission even without specially designed laser cavities. Due to the nonequlibrium carrier distribution among the different confined levels, simultaneous emission on two wavelengths is possible, namely, on the ground state (GS) and the first (or higher) excited state (ES) (Markus et al. 2003; Gioannini 2012; Röhm 2015). See Fig. 1 for a sketch of the energy band structure. In view of the discussion of the previous sections, the possibility for the QD laser to switch to an other optical transition also increases the dynamical degrees of freedom. Compared to single-color lasers, the presence of the second emission wavelength again stabilizes the laser output under delayed feedback. This can be seen in Fig. 10 where we show the dynamic response of the two-state QD laser to optical feedback. There the numerically obtained results for a two-state laser (panel (a)) and an otherwise identical single-color laser (panel (b)) are shown. The regions with pulsations are shown in blue and green, while the intensity of stable cw operation is encoded in orange. In the parameter plane of feedback strength K and feedback phase C, the optical feedback induces complex responses within larger parameter regions for the

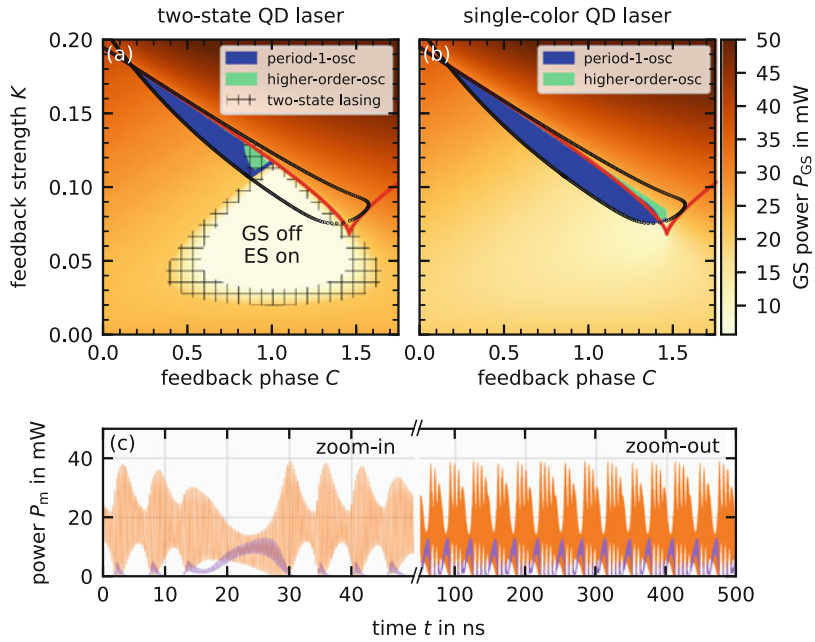

Laser Dynamics and Delayed Feedback, Fig. 10 2D Bifurcation diagram of (**a**): a two state and (**b**): a single color QD laser that is subjected to optical self-feedback. Orange shading indicates the intensity of stable ground state (GS) emission. Blue and green regions indicate regular pulsations and complex dynamics, respectively. Saddle node (SN) and Hopf bifurcations are plotted as red and black lines. (**c**) Time series of the complex dynamics found inside the green region in (**a**), orange and violet show the GS and ES intensity, respectively

single-color QD laser in Fig. 10b. In these parameter regions of complex emission, the two-color laser instead can turn to steady state emission on the excited state (Fig. 10a) and thus can partly suppress the pulsations. The green regions of complex dynamics that occur in the two-color laser are quasi-periodic pulsations that are born in a torus bifurcation. The time evolution of the intensities of the two states is shown in Fig. 10c. Those two-color bursting oscillations are found in regions where the single state QD laser emits chaotic pulse packages as discussed in Fig. 6 in the vicinity of the homoclinic bifurcation. From a dynamic system point of view, the behavior is very interesting as the existence of two-color emission allows for an additional bridge between subsequent ECM, connecting their solutions in parameter space.

Future Directions

The presence of time-delayed feedback in lasers offers a possibility to employ the rich dynamics of delay systems in technological applications. As we have seen, semiconductor lasers with delayed feedback offer a large variety of modes of operation by choice of proper external parameters. Depending on the desired laser behavior, the choice of active medium and cavity design allows control over the susceptibility towards delayed feedback. Only recently the periodic or chaotic dynamics induced by external perturbations such as optical feedback has been seen as an opportunity for novel applications, and not as a nuisance detrimental to the laser operation. A thorough understanding of the material and charge-carrier dynamics in the laser device is crucial for modeling and understanding the complex dynamics that can occur in these laser systems. With quantum-dot lasers and nanolasers, we have illuminated possible material systems for current and future technology where laser dynamics can be employed as an integral part providing the key functionality. Dynamical wavelength switching in QD lasers or the controlled dynamics of nanolasers will possibly allow novel applications in optical computing and data processing. Time-delayed feedback will provide a simple yet effective way of providing the necessary dynamics.

Bibliography

Agrawal GP (1984) Line narrowing in a single-mode injection-laser due to external optical feedback. IEEE

J Quantum Electron 20:468–471. https://doi.org/10.1109/jqe.1984.1072420
Arecchi FT, Lippi GL, Puccioni GP, Tredicce JR (1984) Deterministic chaos in laser with injected signal. Opt Commun 51(5):308–315. https://doi.org/10.1016/0030-4018(84)90016-6
Argyris A, Bueno J, Fischer I (2018) Photonic machine learning implementation for signal recovery in optical communications. Sci Rep 8(8487):1–13. https://doi.org/10.1038/s41598-018-26927-y
Bimberg D, Pohl UW (2011) Quantum dots: promises and accomplishments. Mater Today 14(9):388–397. https://doi.org/10.1016/s1369-7021(11)70183-3
Bimberg D, Grundmann M, Ledentsov NN (1999) Quantum dot heterostructures. Wiley, New York
Binder JO, Cormack GD (1989) Mode selection and stability of a semiconductor laser with weak optical feedback. IEEE J Quantum Electron 25(11):2255. https://doi.org/10.1109/3.42053
Brunner D, Luna R, Latorre ADI, Porte X, Fischer I (2017) Semiconductor laser linewidth reduction by six orders of magnitude via delayed optical feedback. Opt Lett 42(1):163–166. https://doi.org/10.1364/ol.42.000163
Bueno J, Brunner D, Soriano MC, Fischer I (2017) Conditions for reservoir computing performance using semiconductor lasers with delayed optical feedback. Opt Express 25(3):2401–2412. https://doi.org/10.1364/oe.25.002401
Cheng CH, Chen CY, Chen JD, Pan DK, Ting KT, Lin FY (2018) 3d pulsed chaos lidar system, Opt Express 26(9):12230–12241. https://doi.org/10.1364/oe.26.012230
Choi D, Wishon MJ, Viktorov EA, Citrin DS, Locquet A (2019) Nanometric sensing with laser feedback interferometry. Opt Lett 44(4):903–906. https://doi.org/10.1364/ol.44.000903
Chow WW, Koch SW (1999) Semiconductor-laser fundamentals. Springer, Berlin
Duan J, Huang H, Dong B, Jung D, Norman JC, Bowers JE, Grillot F (2019) 1.3-μ m reflection insensitive inas/gaas quantum dot lasers directly grown on silicon. IEEE Photon Technol Lett 31(5):345–348. https://doi.org/10.1109/lpt.2019.2895049
Erneux T, Rogister F, Gavrielides A, Kovanis V (2000) Bifurcation to mixed external cavity mode solutions for semiconductor lasers subject to optical feedback. Opt Commun 183(5–6):467–477. https://doi.org/10.1016/s0030-4018(00)00899-3
Erneux T, Javaloyes J, Wolfrum M, Yanchuk S (2017) Introduction to focus issue: time-delay dynamics. Chaos 27(11):114201. https://doi.org/10.1063/1.5011354
Flunkert V, Schöll E (2007) Suppressing noise-induced intensity pulsations in semiconductor lasers by means of time-delayed feedback. Phys Rev E 76:066202. https://doi.org/10.1103/physreve.76.066202
Gioannini M (2012) Ground-state quenching in two-state lasing quantum dot lasers. J Appl Phys 111:043108. https://doi.org/10.1063/1.3682574
Globisch B, Otto C, Schöll E, Lüdge K (2012) Influence of carrier lifetimes on the dynamical behavior of quantum-dot lasers subject to optical feedback. Phys Rev E 86:046201. https://doi.org/10.1103/physreve.86.046201
Haken H (1986) Laser light dynamics, vol II, 1st edn. North Holland, Amsterdam
Heil T, Fischer I, Elsäßer W, Gavrielides A (2001) Dynamics of semiconductor lasers subject to delayed optical feedback: the short cavity regime. Phys Rev Lett 87:243901. https://doi.org/10.1103/physrevlett.87.243901
Heil T, Fischer I, Elsäßer W, Krauskopf B, Green K, Gavrielides A (2003) Delay dynamics of semiconductor lasers with short external cavities: bifurcation scenarios and mechanisms. Phys Rev E 67:066214. https://doi.org/10.1103/physreve.67.066214
Helms J, Petermann K (1990) A simple analytic expression for the stable operation range of laser diodes with optical feedback. IEEE J Quantum Electron 26(5):833. https://doi.org/10.1109/3.55523
Huyet G, O'Brien D, Hegarty SP, McInerney JG, Uskov AV, Bimberg D, Ribbat C, Ustinov VM, Zhukov AE, Mikhrin SS, Kovsh AR, White JK, Hinzer K, SpringThorpe AJ (2004) Quantum dot semiconductor lasers with optical feedback. Phys Status Solidi B 201(2): 345–352. https://doi.org/10.1002/pssa.200303971
Jaurigue LC, Schöll E, Lüdge K (2016) Suppression of noise-induced modulations in multidelay systems. Phys Rev Lett 117:154101. https://doi.org/10.1103/physrevlett.117.154101
Jüngling T, Soriano MC, Oliver N, Porte X, Fischer I (2018) Consistency properties of chaotic systems driven by time-delayed feedback. Phys Rev E 97:042202. https://doi.org/10.1103/physreve.97.042202
Kane DM, McMahon C, Argyris A, Syvridis D (2015) Integrated semiconductor laser with optical feedback: transition from short to long cavity regime. Opt Express 23(14):18754. https://doi.org/10.1364/oe.23.018754
Karsaklian Dal A, Bosco S, Ohara N, Sato Y, Akizawa A, Uchida T, Harayama MI (2017) Dynamics versus feedback delay time inphotonic integrated circuits: mapping theshort cavity regime. IEEE Photon J 9(2):1. https://doi.org/10.1109/jphot.2017.2667883
Kim B, Locquet A, Li N, Choi D, Citrin DS (2014) Bifurcation-cascade diagrams of an external-cavity semiconductor laser: experiment and theory. IEEE J Quantum Electron 50(12):965–972. https://doi.org/10.1109/jqe.2014.2363568
Kuriki Y, Nakayama J, Takano K, Uchida A (2018) Impact of input mask signals on delay-based photonic reservoir computing with semiconductor lasers. Opt Express 26(5):5777–5788. https://doi.org/10.1364/oe.26.005777
Lang R, Kobayashi K (1980) External optical feedback effects on semiconductor injection laser properties. IEEE J Quantum Electron 16:347–355. https://doi.org/10.1109/jqe.1980.1070479
Lenstra D, Verbeek B, Den Boef A (1985) Coherence collapse in single-mode semiconductor lasers due to optical feedback. IEEE J Quantum Electron 21(6):674–679. https://doi.org/10.1109/jqe.1985.1072725
Lenstra D, van Schaijk TTM, Williams KA (2019) Toward a feedback-insensitive semiconductor laser. IEEE J Sel

Top Quantum Electron 25(6):1. https://doi.org/10.1109/jstqe.2019.2924139
Levine AM, van Tartwijk GHM, Lenstra D, Erneux T (1995) Diode lasers with optical feedback: stability of the maximum gain mode. Phys Rev A 52(5):R3436. https://doi.org/10.1103/physreva.52.r3436. (4 pages)
Li H, Ye J, McInerney JG (1993) Detailed analysis of coherence collapse in semiconductor lasers. IEEE J Quantum Electron 29(9):2421–2432. https://doi.org/10.1109/3.247700
Lin FY, Liu JM (2004) Chaotic LIDAR. IEEE J Sel Top Quantum Electron 10(5):991–997. https://doi.org/10.1109/jstqe.2004.835296
Lindner B, García-Ojalvo J, Neiman AB, Schimansky-Geier L (2004) Effects of noise in excitable systems. Phys Rep 392:321–424. https://doi.org/10.1016/j.physrep.2003.10.015
Lingnau B (2015) Nonlinear and nonequilibrium dynamics of quantum-dot optoelectronic devices. Springer Theses (Springer International Publishing), Cham. https://doi.org/10.1007/978-3-319-25805-8
Lingnau B, Lüdge K, Chow WW, Schöll E (2012) Failure of the α-factor in describing dynamical instabilities and chaos in quantum-dot lasers. Phys Rev E 86(6):065201(R). https://doi.org/10.1103/physreve.86.065201
Lingnau B, Chow WW, Schöll E, Lüdge K (2013) Feedback and injection locking instabilities in quantum-dot lasers: a microscopically based bifurcation analysis. New J Phys 15:093031. https://doi.org/10.1088/1367-2630/15/9/093031
Lingnau B, Turnwald J, Lüdge K (2019) Class-C semiconductor lasers with time-delayed optical feedback. Phil Trans R Soc A 377(2153):20180124. https://doi.org/10.1098/rsta.2018.0124
Locquet A, Kim B, Choi D, Li N, Citrin DS (2017) Initial-state dependence of the route to chaos of an external-cavity laser. Phys Rev A 95:023801. https://doi.org/10.1103/physreva.95.023801
Lüdge K, Schöll E (2009) Quantum-dot lasers – desynchronized nonlinear dynamics of electrons and holes. IEEE J Quantum Electron 45(11):1396–1403. https://doi.org/10.1109/jqe.2009.2028159
Markus A, Chen JX, Paranthoen C, Fiore A, Platz C, Gauthier-Lafaye O (2003) Simultaneous two-state lasing in quantum-dot lasers. Appl Phys Lett 82(12):1818. https://doi.org/10.1063/1.1563742
Mørk J, Tromborg B, Christiansen PL (1988a) Bistability and low-frequency fluctuations in semiconductor lasers with optical feedback: a theoretical analysis. IEEE J Quantum Electron 24(2):123–133. https://doi.org/10.1109/3.105
Mørk J, Christiansen PL, Tromborg B (1988b) Limits of stable operation of ar-coated semiconductor lasers with strong optical feedback. Electron Lett 24(17):1065. https://doi.org/10.1049/el:19880722
Mørk J, Mark J, Tromborg B (1990a) Route to chaos and competition between relaxation oscillations for a semiconductor laser with optical feedback. Phys Rev Lett 65(16):1999–2002. https://doi.org/10.1103/physrevlett.65.1999
Mørk J, Semkow M, Tromborg B (1990b) Measurement and theory of mode hopping in external cavity lasers. Electron Lett 26(9):609–610. https://doi.org/10.1049/el:19900400
Mørk J, Tromborg B, Mark J (1992) Chaos in semiconductor lasers with optical feedback-theory and experiment. IEEE J Quantum Electron 28:93–108. https://doi.org/10.1109/3.119502
Nguimdo RM, Lacot E, Jacquin O, Hugon O, Van der Sande G, de Chatellus HG (2017) Prediction performance of reservoir computing systems based on a diode-pumped erbium-doped microchip laser subject to optical feedback. Opt Lett 42(3):375. https://doi.org/10.1364/ol.42.000375
O'Brien D, Hegarty SP, Huyet G, Uskov AV (2004) Sensitivity of quantum-dot semiconductor lasers to optical feedback. Opt Lett 29(10):1072–1074. https://doi.org/10.1364/ol.29.001072
Ohtsubo J (1999) Feedback induced instability and chaos in semiconductor lasers and their applications. J Opt Rev 6:1–15. https://doi.org/10.1007/s10043-999-0001-z
Ohtsubo J (2013) Semiconductor lasers: stability, instability and chaos, 3rd edn. Springer, Berlin. https://doi.org/10.1007/978-3-642-30147-6
Olejniczak L, Sciamanna M, Thienpont H, Panajotov K, Mutig A, Hopfer F, Bimberg D (2009) Polarization switching in quantum-dot vertical-cavity surface-emitting lasers. IEEE Photon Technol Lett 21(14):1008–1010. https://doi.org/10.1109/lpt.2009.2021954
Oliver N, Soriano MC, Sukow DW, Fischer I (2011) Dynamics of a semiconductor laser with polarization-rotated feedback and its utilization for random bit generation. Opt Lett 36(23):4632–4634. https://doi.org/10.1364/ol.36.004632
Oliver N, Jüngling T, Fischer I (2015) Consistency properties of a chaotic semiconductor laser driven by optical feedback. Phys Rev Lett 114(123902):114. https://doi.org/10.1103/physrevlett.114.123902
Osborne S, Buckley K, Amann A, O'Brien S (2009) All-optical memory based on the injection locking bistability of a two-color laser diode. Opt Express 17(8):6293–6300. https://doi.org/10.1364/oe.17.006293
Osborne S, Heinricht P, Brandonisio N, Amann A, O'Brien S (2012) Wavelength switching dynamics of two-colour semiconductor lasers with optical injection and feedback. Semicond Sci Technol 27(9):094001. https://doi.org/10.1088/0268-1242/27/9/094001
Otto C, Lüdge K, Schöll E (2010) Modeling quantum dot lasers with optical feedback: sensitivity of bifurcation scenarios. Phys Status Solidi B 247(4):829–845. https://doi.org/10.1002/pssb.200945434
Otto C, Globisch B, Lüdge K, Schöll E, Erneux T (2012a) Complex dynamics of semiconductor quantum dot lasers subject to delayed optical feedback. Int J Bifurc Chaos 22(10):1250246. https://doi.org/10.1142/s021812741250246x
Otto C, Lüdge K, Viktorov EA, Erneux T (2012b) Quantum dot laser tolerance to optical feedback. In: Lüdge K (ed) Nonlinear laser dynamics – from quantum dots to cryptography. Wiley-VCH, Weinheim, pp 141–162

Otto C, Lingnau B, Schöll E, Lüdge K (2014) Manipulating coherence resonance in a quantum dot semiconductor laser via electrical pumping. Opt Express 22:13288. https://doi.org/10.1364/oe.22.013288

Otto A, Just W, Radons G (2019) Nonlinear dynamics of delay systems: an overview. Phil Trans R Soc A 377(2153):20180389. https://doi.org/10.1098/rsta.2018.0389

Pieroux D, Erneux T, Gavrielides A, Kovanis V (2000) Hopf bifurcation subject to a large delay in a laser system. SIAM J Appl Math 61(3):966–982. https://doi.org/10.1137/s0036139999360131

Pieroux D, Erneux T, Haegeman B, Engelborghs K, Roose D (2001) Bridges of periodic solutions and tori in semiconductor lasers subject to delay. Phys Rev Lett 87(19):193901. https://doi.org/10.1103/physrevlett.87.193901

Porte X, Soriano MC, Fischer I (2014) Similarity properties in the dynamics of delayedfeedback semiconductor lasers. Phys Rev A 89:023822. https://doi.org/10.1103/physreva.89.023822

Radziunas M, Wünsche HJ, Krauskopf B (2006) External cavity modes in Lang-Kobayashi and travelling wave models. M Wolfrum Proc SPIE 6184:61840X. https://doi.org/10.1117/12.663546

Reidler I, Aviad Y, Rosenbluh M, Kanter I (2009) Ultrahigh-speed random number generation based on a chaotic semiconductor laser. Phys Rev Lett 103:024102. https://doi.org/10.1103/physrevlett.103.024102

Röhm A (2015) Dynamic scenarios in two-state quantum dot lasers. BestMasters 2015. Springer Spektrum, Wiesbaden. https://doi.org/10.1007/978-3-658-09402-7

Röhm A, Lingnau B, Lüdge K (2015) Understanding ground-state quenching in quantum-dot lasers. IEEE J Quantum Electron 51(1):2000211. https://doi.org/10.1109/jqe.2014.2370793

Rontani D, Locquet A, Sciamanna M, Citrin DS (2007) Loss of time-delay signature in the chaotic output of a semiconductor laser with optical feedback. Opt Lett 32(20):2960–2962. https://doi.org/10.1364/ol.32.002960

Rontani D, Locquet A, Sciamanna M, Citrin DS, Ortin S (2009) Time-delay identification in a chaotic semiconductor laser with optical feedback: a dynamical point of view. IEEE J Quantum Electron 45(7):879–1891. https://doi.org/10.1109/jqe.2009.2013116

Rosanov NN (1975) Kinetics of a solid-state laser with an additional moving mirror. Sov J Quant Electron 4(10):1191–1193. https://doi.org/10.1070/qe1975v004n10abeh011629

Rottschäfer V, Krauskopf B (2007) The ECM-backbone of the Lang-Kobayashi equations: a geometric picture. Int J Bifurc Chaos 17(5):1575–1588. https://doi.org/10.1142/s0218127407017914

Sano T (1994) Antimode dynamics and chaotic itinerancy in the coherence collapse of semiconductor lasers with optical feedback. Phys Rev A 50(3):2719–2726. https://doi.org/10.1103/physreva.50.2719

Schelte C, Camelin P, Marconi M, Garnache A, Huyet G, Beaudoin G, Sagnes I, Giudici M, Javaloyes J, Gurevich SV (2019) Third order dispersion in time-delayed systems. Phys Rev Lett 123:043902. https://doi.org/10.1103/physrevlett.123.043902

Sciamanna M, Panajotov K, Thienpont H, Veretennicoff I, Mégret P, Blondel M (2003) Optical feedback induces polarization mode hopping in vertical-cavity surface-emitting lasers. Opt Lett 28(17):1543–1545. https://doi.org/10.1364/ol.28.001543

Simmendinger C, Hess O (1996) Controlling delay-induced chaotic behavior of a semiconductor laser with optical feedback. Phys Lett A 216:97. https://doi.org/10.1016/0375-9601(96)00269-1

Soriano MC, García-Ojalvo J, Mirasso CR, Fischer I (2013) Complex photonics: Dynamics and applications of delay-coupled semiconductors lasers. Rev Mod Phys 85:421–470. https://doi.org/10.1103/revmodphys.85.421

van Tartwijk GHM, Agrawal GP (1998) Laser instabilities: a modern perspective. Prog Quantum Electron 22(2):43–122. https://doi.org/10.1016/s0079-6727(98)00008-1

Verschaffelt G, Khoder M, Van der Sande G (2017) Random number generator based on an integrated laser with on-chip optical feedback. Chaos 27(11):114310. https://doi.org/10.1063/1.5007862

Virte M, Panajotov K, Thienpont H, Sciamanna M (2012) Deterministic polarization chaos from a laser diode. Nat Photonics 7(1):60–65. https://doi.org/10.1038/nphoton.2012.286

Wolfrum M, Turaev DV (2002) Instabilities of lasers with moderately delayed optical feedback. Opt Commun 212(1–3): 127–138. https://doi.org/10.1016/s0030-4018(02)01824-2

Wünsche HJ, Schikora S, Henneberger F (2008) Noninvasive Control of Semiconductor Lasers by Delayed Optical Feedback. In: Schuster HG, Schöll E (eds) Handbook of chaos control. Wiley-VCH, Weinheim. https://doi.org/10.1002/9783527622313.ch21. Second completely revised and enlarged edition

Yanchuk S, Perlikowski P (2009) Delay and periodicity. Phys Rev E 79(4):046221. https://doi.org/10.1103/physreve.79.046221

Yanchuk S, Wolfrum M (2004) Instabilities of stationary states in lasers with long-delay optical feedback. Rep Weierstrass Inst Appl Anal Stochastics 962:1–16

Ye SY, Ohtsubo J (1998) Experimental investigation of stability enhancement in semiconductor lasers with optical feedback. Opt Rev 5(5):280–284. https://doi.org/10.1007/s10043-998-0280-9